

Precipitation behavior of BN type inclusions in 42CrMo steel

Yu-nan Wang^{1,2)}, Yan-ping Bao^{1,2)}, Min Wang³⁾, and Le-chen Zhang^{1,2)}

1) State Key Laboratory of Advanced Metallurgy, University of Science and Technology Beijing, Beijing 100083, China

2) School of Metallurgical and Ecological Engineering, University of Science and Technology Beijing, Beijing 100083, China

3) National Engineering Research Center of Flat Rolling Equipment, University of Science and Technology Beijing, Beijing 100083, China

(Received: 19 February 2012; revised: 15 March 2012; accepted: 7 April 2012)

Abstract: Automobile crankshaft steel 42CrMo, which requires excellent machinability and mechanical properties, cannot be manufactured by traditional methods. To achieve these qualities, the formation behavior of boron nitride (BN) inclusions in 42CrMo steel was studied in this article. First, the precipitation temperature and the amount of BN type inclusions with different contents of boron and nitrogen in molten steel were calculated thermodynamically by FactSage software. Then the morphology and the size of BN type inclusions as well as the influence of cooling methods on them were investigated by scanning electron microscopy. Furthermore, the effects of cooling rate and the contents of B and N in molten steel on the morphology, size, and distribution of BN type inclusions were studied quantitatively and detailedly by directional solidification experiments. It is found that different BN inclusions in molten steel can form by controlling the cooling rate and the contents of B and N, which is important for obtaining the excellent machinability of 42CrMo steel.

Keywords: steel; solidification; boron nitride; inclusions; precipitation

1. Introduction

Free cutting steels used for mechanical structures are often produced by adding sulfur or lead. Lead series free cutting steel has been widely used for its best cutting performance, such as tool life, chip disposability, and surface finish. However, because of lead pollution to the environment and its harmful effects on the process of scrap recycling, its application has been limited, and the recycle of leaded auto parts has been forbidden by the European Community Regulations. Therefore, it is necessary to develop new non-leaded free cutting steels.

Boron nitride (BN) free-cutting steel is a response to this trend. Since BN has a hexagonal crystal structure similar to graphite, whose hexagonal layered structure can be cut easily, it can improve the free cutting property of steel during the deformation process at high temperature. BN free-cutting steel has a better free cutting property than lead-free free-cutting steel when it is used for mechanical structures, and has better mechanical properties than leaded, phosphorus, and sulfur free-cutting steel. It also has a better ma-

chinability in the field of high-speed cutting and has the same cold ductility as low carbon steel. BN free-cutting steel has good cold forming and cutting performances, which had been considered impossible previously. In recent years, Tanaka *et al.* [1-5] carried out the exploration to improve the free cutting property of steel through crystallizing out BN type inclusions in steel and controlled the mode of sulfide species by adjusting the steel composition. However, the development of BN free-cutting steel has not been reported in China. The improvement of free-cutting property depends on the type, shape, size, amount, and distribution of inclusions in steel [6], thus the precipitation behavior of BN type inclusions in 42CrMo steel was studied in this paper.

2. Experimental material and methods

2.1. Experimental material

The experimental material was a 42CrMo round billet with a size of $\phi 36 \text{ mm} \times 650 \text{ mm}$, and the chemical composition is listed in Table 1.

Corresponding author: Yan-ping Bao E-mail: baoy@ustb.edu.cn

© University of Science and Technology Beijing and Springer-Verlag Berlin Heidelberg 2013

Table 1. Chemical composition of the experimental material

| | | | | | | | | | | wt% |
|-----------|-----------|-----------|--------|--------|-------------|-----------|-------|-------|-----------|-----|
| C | Si | Mn | P | S | N | Cr | Ni | Cu | Mo | |
| 0.38-0.45 | 0.17-0.37 | 0.50-0.80 | ≤0.035 | ≤0.035 | 0.0097-0.01 | 0.90-1.20 | ≤0.25 | ≤0.20 | 0.15-0.25 | |

2.2. Experimental methods

Cold crucible induction melting experiments were conducted in a tubular resistance furnace to produce BN samples. A crucible with a capacity of 1 kg steel (purity: 99.99% Al_2O_3) was used. The whole experimental process was protected by nitrogen (2 L/min), and the temperature was controlled in the range of 1620-1650°C. The experimental process was as the follows. The crucible containing 1 kg 42CrMo steel was placed in the resistance furnace, and ohmic heating was carried out until the steel was melted and the required temperature was achieved. Ferro boron (the content of boron is about 20wt%) and nitrogen were added according to different ratios of N/B, and finally the samples with different contents of B and N were prepared. The cooling methods of samples were divided into water quenching, air cooling, furnace cooling, and controlled cooling (Fig. 1). The composition and morphology of BN type inclusions in the samples were observed by a scanning electron microscope (SEM, Zeiss Ultra55) with energy dispersive spectroscopy (EDS, Oxford Instruments Inca X-max50) after being lapped and polished, and the number of BN type inclusions in different particle sizes per unit area was counted. Meanwhile, FactSage software was used to calculate the precipitation of BN type inclusions in steel that had different contents of B and N in thermodynamic equilibrium state, which provides a verification and theoretical basis for the experiment.

In order to further study the effects of cooling rate and the contents of B and N in molten steel on the morphology, size, and distribution of BN type inclusions, four samples with different contents of B and N were selected for directional solidification experiments. Based on the requirement of directional solidification

experiments, the samples were prepared for smooth bars with a size of $\phi 6.5 \text{ mm} \times 100 \text{ mm}$. The experimental equipment was a Bridgman directional solidification system. The heating method was induction heating, and it depended on a graphite heater which was heated by an induction coil to heat alloys by heat transfer. The temperature gradient G was $5.2 \times 10^3 \text{ }^\circ\text{C/m}$ [7], and the withdrawal rates were 10 and 1000 $\mu\text{m/s}$, respectively. Under this condition, eight directional solidification samples were obtained. The composition and morphology of BN type inclusions in the samples that had been polished and lapped were observed by SEM, and the amount of BN type inclusions in different particle size ranges per unit area was counted.

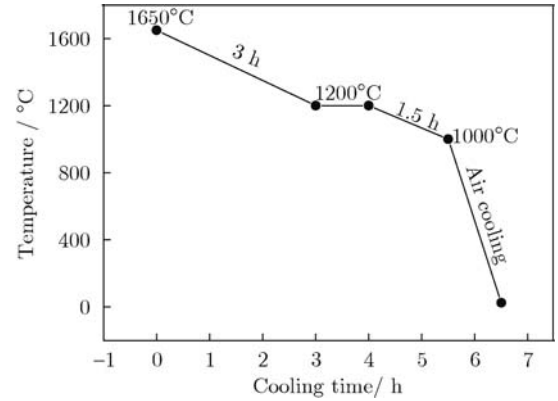


Fig. 1. Controlled cooling curve.

3. Results and discussion

3.1. Results of smelting experiments

The chemical composition of the samples obtained by cold crucible induction melting is shown in Table 2.

Table 2. Chemical composition of the samples

| | | | | | | | | | | wt% |
|--------|-------|-------|-------|-------|-------|-------|-------|--------|--------|-------|
| Sample | C | Si | Mn | P | S | O | Ti | Sol.Al | B | N |
| BN1 | 0.420 | 0.362 | 0.781 | 0.017 | 0.018 | 0.005 | 0.052 | 0.031 | 0.0890 | 0.041 |
| BN2 | 0.420 | 0.362 | 0.781 | 0.017 | 0.018 | 0.005 | 0.052 | 0.031 | 0.0890 | 0.032 |
| BN3 | 0.420 | 0.362 | 0.781 | 0.017 | 0.018 | 0.005 | 0.052 | 0.031 | 0.0109 | 0.043 |
| BN4 | 0.420 | 0.362 | 0.781 | 0.017 | 0.018 | 0.005 | 0.052 | 0.031 | 0.0250 | 0.042 |
| BN5 | 0.420 | 0.362 | 0.781 | 0.017 | 0.018 | 0.005 | 0.052 | 0.031 | 0.0044 | 0.030 |
| BN6 | 0.420 | 0.362 | 0.781 | 0.017 | 0.018 | 0.005 | 0.052 | 0.031 | 0.0150 | 0.043 |

Note: Sol.Al — Acid-soluble aluminium.

Cooling methods were different for different samples. Samples BN1-4 were natural cooling, sample BN5 was water quenching, and cooling methods for sample BN6 were air cooling, furnace cooling, and controlled cooling.

3.2. Calculation results by FactSage software

The relationship between the precipitation of BN

type inclusions and temperature, which was calculated by FactSage software in thermal equilibrium state, is shown in Fig. 2 (supposing that the molten steel was 100 g). The precipitation amount and temperature are shown in Table 3. With different contents of B and N, the amount, temperature, and change law of the precipitation of BN type inclusions are different.

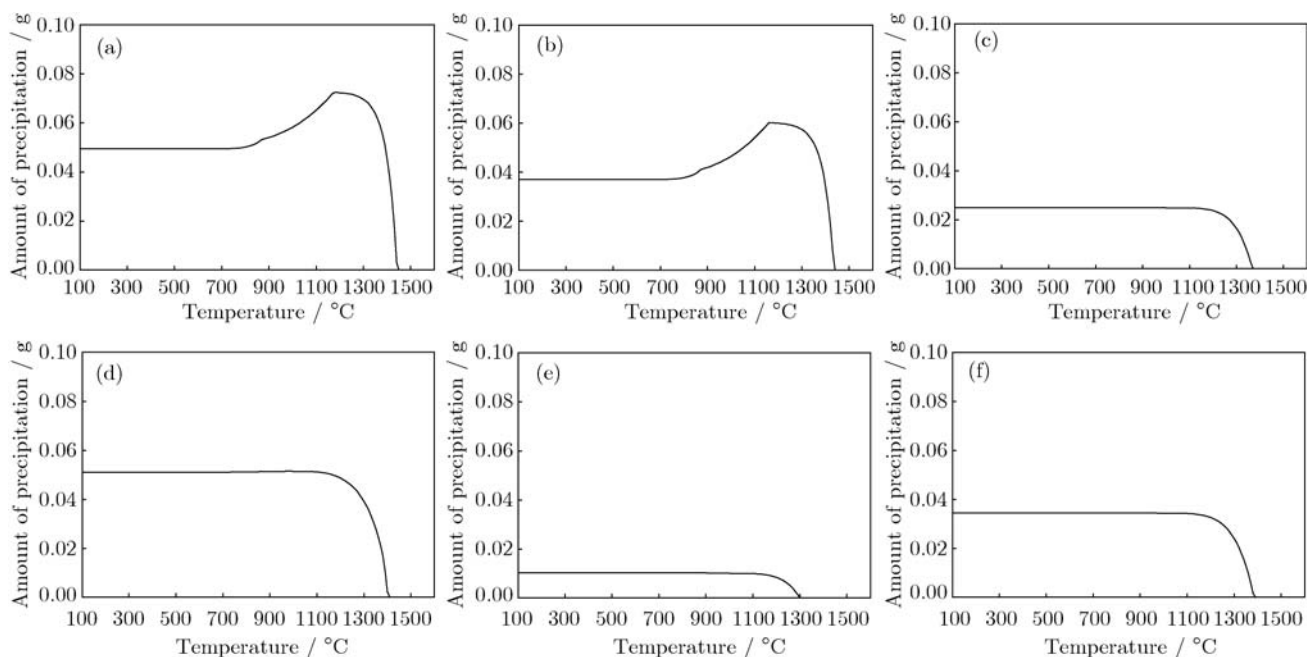


Fig. 2. Relationship between the precipitation amount and temperature of different BN type inclusions: (a) BN1; (b) BN2; (c) BN3; (d) BN4; (e) BN5; (f) BN6.

Table 3. Calculation results of the precipitation amount and temperature of BN type inclusions

| Sample | Contents of B and N in molten steel / wt% | | Maximum precipitation amount / g | Final precipitation amount / g | Starting precipitation temperature / °C |
|--------|---|-------|----------------------------------|--------------------------------|---|
| | B | N | | | |
| BN1 | 0.0890 | 0.041 | 0.0724 | 0.0493 | 1440 |
| BN2 | 0.0890 | 0.034 | 0.0601 | 0.0368 | 1430 |
| BN3 | 0.0109 | 0.043 | 0.0250 | 0.0250 | 1360 |
| BN4 | 0.0250 | 0.042 | 0.0528 | 0.0511 | 1400 |
| BN5 | 0.0044 | 0.030 | 0.0101 | 0.0101 | 1290 |
| BN6 | 0.0150 | 0.043 | 0.0344 | 0.0344 | 1380 |

As shown in Fig. 2 and Table 3, in thermal equilibrium state, the maximum precipitation amount, the final precipitation amount, and the starting precipitation temperature of BN type inclusions are determined by the B and N contents in steel. The calculation results of samples BN1 and BN2 show that when the B content is constant in steel, the maximum precipitation amount, the final precipitation amount, and the starting precipitation temperature of BN type inclu-

sions will increase with the increase in N content in steel. Comparing the calculation results of samples BN3 and BN6, it is known that when the N content is constant in steel, they will increase with the increase in B content. The precipitation amount of BN type inclusions in samples BN1 and BN2 decreases near 800°C (Figs. 2(a) and 2(b)). Since nitrogen is easy to react with Al and Ti in molten steel, N in BN inclusions is probably taken away by Ti and Al, and free B

is left in the two samples. As shown in Figs. 2(c), 2(e), and 2(f), N is enough to react with B, and there is no free B left in the samples. Fig. 2(d) shows that the precipitation amount of BN inclusions is up to the maximum and declines a little; it means that the reaction of B and N is almost complete. The N/B ratio is about 1.7 when the reaction of B and N is complete in 42CrMo steel. The rapid precipitation temperature of BN type inclusions is about 1300-1400°C, therefore, in order to control the precipitation of BN inclusions, the heat treatment temperature is about in this range.

In previous researches [8-9], the precipitation temperature of BN type inclusions in heat resistant steel, which is about between 1150 and 1200°C (B: 0.003wt%; N: 0.06wt%), is similar to the calculation results, and it confirms that the calculation results are similar to the practical precipitation behavior of BN type inclusions. From the thermodynamic perspective, the solid solubility formula of various nitrides in molten steel can be expressed by Eqs. (1)-(3) [10]:

$$\lg\{[Al][N]\}_{\gamma}=1.79-7184/T \quad (1)$$

$$\lg\{[Ti][N]\}_{\gamma}=0.32-8000/T \quad (2)$$

$$\lg\{[B][N]\}_{\gamma}=4.160-14694/T \quad (3)$$

where [Al], [Ti], [B], and [N] are the contents of Al, Ti, B, and N in molten steel, respectively; and T is the temperature, K.

When the contents of Al, Ti, and B are the same in molten steel, the precipitation order is BN, TiN, and AlN. However, the Ti content is more than the B content in these samples, so the precipitation of TiN would be priority to BN.

From the perspective of kinetics, B has a slightly higher diffusion coefficient than N and is ten times of Al [11-12], so the growth of BN type inclusions is determined by the diffusion of N, meanwhile, the precipitation of AlN has been repressed gravely by B in samples. In our research, AlN was not found. In practical production, B combines with free N preferentially to form coarse BN particles in molten steel. When MnS exists in molten steel, the intragranular precipitation of BN type inclusions take precedence over grain boundaries, so BN type inclusions could be easily separated with MnS [11, 13-14]. This research also confirms the conclusion.

3.3. Morphology and size of BN type inclusions

Typical BN type inclusions in the samples are shown in Fig. 3, and there are mainly single BN type inclusions and complex inclusions composited with Al_2O_3 , MnS, and TiN. BN type inclusions separate from Al_2O_3 , MnS, and TiN to all or unilateral direction as Al_2O_3 , MnS, and TiN nucleus, sometimes three and more precipitates would appear with BN together. The size of BN type inclusions is from 5 to 50 μm .

Surface scan of typical BN type inclusions in the samples is shown in Figs. 4-6. From the following

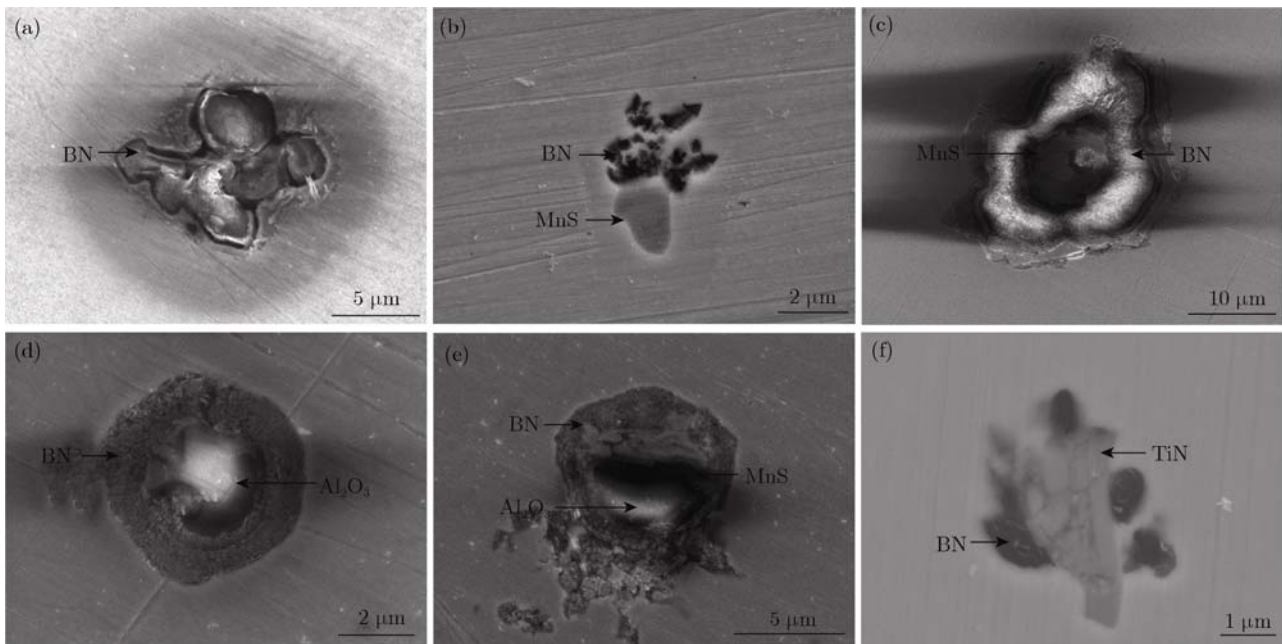


Fig. 3. Morphologies of single BN type inclusions (a) and composite BN type inclusions in the samples: (b), (c) with MnS; (d) with Al_2O_3 ; (e) with Al_2O_3 and MnS; (f) with TiN.

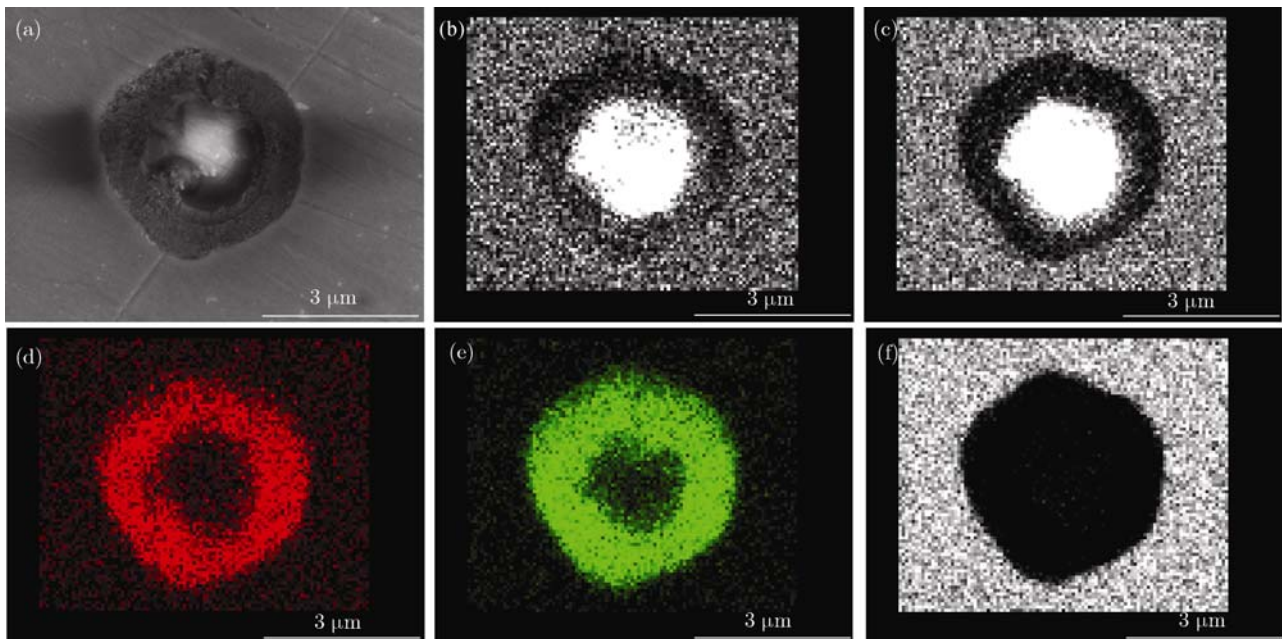


Fig. 4. Morphology (a) and element distribution of typical BN type inclusions in the samples (composited with Al_2O_3): (b) Al; (c) O; (d) B; (e) N; (f) Fe.

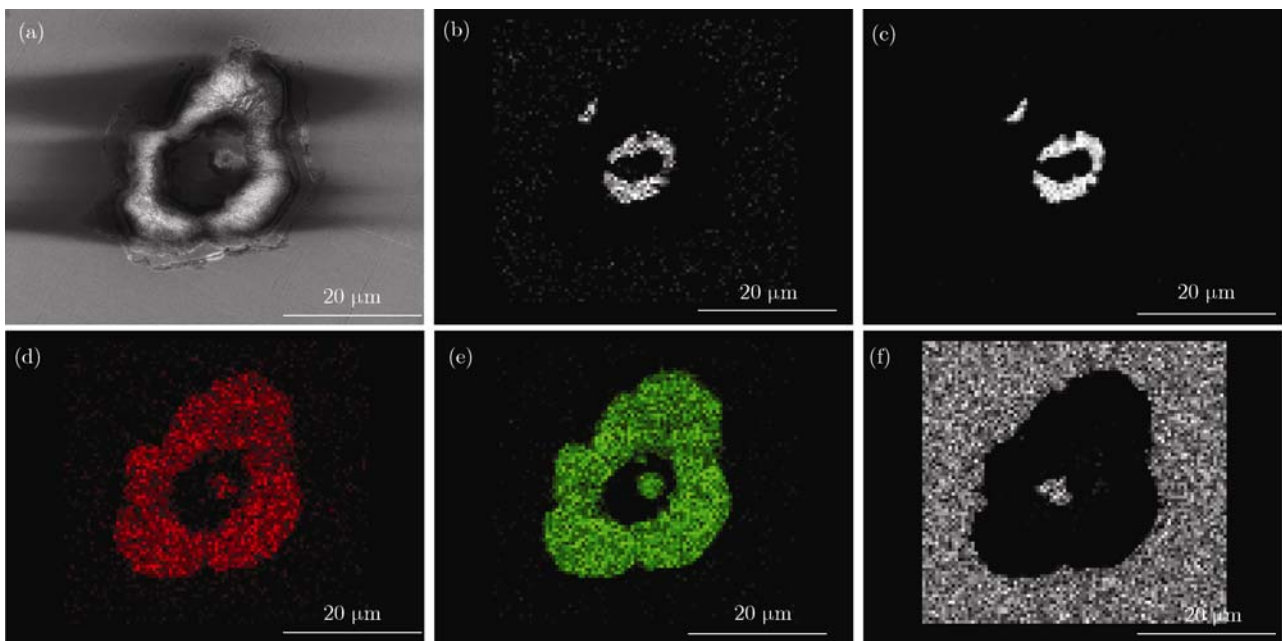


Fig. 5. Morphology (a) and element distribution of typical BN type inclusions in the samples (composited with MnS): (b) Mn; (c) S; (d) B; (e) N; (f) Fe.

graphs, it could be observed that BN type inclusions separate out from Al_2O_3 , MnS, and TiN to all or unilateral direction as Al_2O_3 , MnS, and TiN nucleus. When BN diffuses uniformly, the shape is spherical; otherwise, the shape is spindle or irregular polygon. The composite precipitation of MnS and Al_2O_3 as the nucleus exists.

The morphology and the size of BN type inclusions in the samples are determined by cooling methods, as shown in Table 4. Some previous researches [8-11] showed that the size of BN type inclusions was inversely proportional to the cooling rate, and this paper also confirmed that opinion.

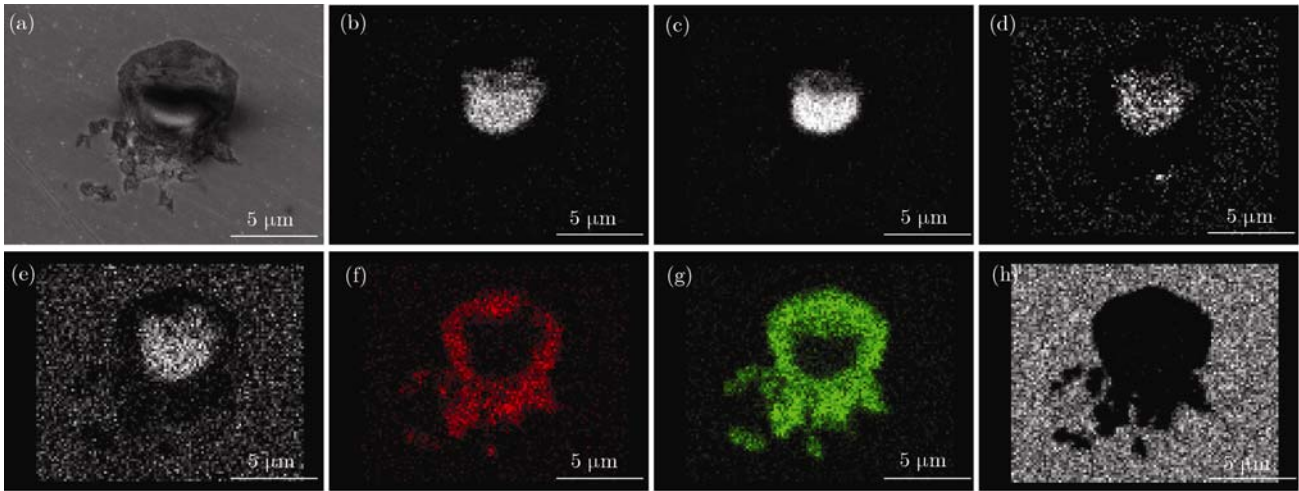


Fig. 6. Morphology (a) and element distribution of typical BN type inclusions in the samples (composed with Al₂O₃ and MnS): (b) Al; (c) O; (d) Mn; (e) S; (f) B; (g) N; (h) Fe.

Table 4. Morphology and size of BN type inclusions with different cooling methods

| Cooling method | Size / μm | | Morphology | |
|--------------------|----------------------|--------------|------------------------------|-------------------------|
| | Single BN | Composite BN | Single BN | Composite BN |
| Water quenching | Not found | Not found | Not found | Not found |
| Air cooling | 1-20 | 5-20 | Spherical, irregular polygon | Near spherical, spindle |
| Furnace cooling | 10-50 | 10-50 | Spherical, lumpy | Near spherical, lumpy |
| Controlled cooling | 20-50 | 20-50 | Spherical | Near spherical |

As shown in Table 4, cooling methods have tremendous impact on the morphology and size of BN type inclusions. Cooling methods for sample BN6 are divided into natural cooling, furnace cooling, and controlled cooling. The size of BN type inclusions affected by cooling methods could be observed by analyzing sample BN6 (Fig. 7). It clearly shows that as the cooling rate increases, the number of large-size particles decreases, and the number of small-size particles increases. The calculation by FactSage software showed that the rapid precipitation temperature of BN type inclusions is about 1300-1400°C. When the cooling method is water quenching, the cooling rate is too rapid for BN type inclusions to separate out, so B and N have a large super saturation in molten steel. Similarly, when the cooling method is natural cooling, B and N have high diffusion rates at high temperature; as a result, a large number of fine BN particles are thought to precipitate. However, the cooling rate is still too fast, BN particles do not have enough time to grow up, which causes the small size of BN type inclusions. On the contrary, furnace cooling and controlled cooling have enough time to make BN type inclusions

grow up. Especially for controlled cooling, because the temperature stays at 1200°C when BN type inclusions are precipitated, the amount and size of BN type inclusions in the sample are both larger.

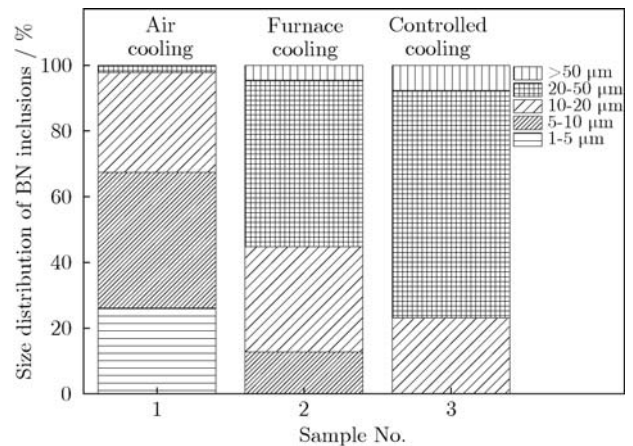


Fig. 7. Size distribution of BN type inclusions in sample BN6 with different cooling methods.

The size of BN type inclusions affected by the contents of B and N in molten steel is shown in Fig. 8, in

which four samples were cooled by natural cooling. It shows that at the same cooling rate, the contents of B and N could hardly affect the size of BN type inclusions.

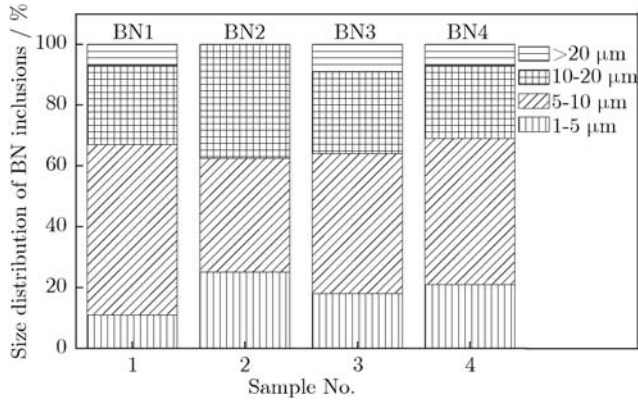


Fig. 8. Size distribution of BN type inclusions in air cooling samples with different contents of B and N.

3.4. Results and analysis of directional solidification

The above study proved that the morphology and size of BN type inclusions in the samples are affected by cooling rate. To obtain the precipitation law of BN type inclusions, directional solidification was implemented. The sample number and chemical composition of directional solidification specimens are shown in Table 5. The cooling rate can be calculated by

$$R = Gv \quad (4)$$

where R is the cooling rate, °C/s; G the temperature gradient, K·m⁻¹; and v the withdrawal rate, m·s⁻¹.

Table 5. Sample number and chemical composition of directional solidification specimens

| Sample No. | Sample | Cooling rate / (°C·s ⁻¹) | B content / wt% | N content / wt% |
|------------|--------|--------------------------------------|-----------------|-----------------|
| 1 | BN8 | 5.2 | 0.0110 | 0.040 |
| 2 | BN9 | 5.2 | 0.0150 | 0.042 |
| 3 | BN10 | 5.2 | 0.0038 | 0.034 |
| 4 | BN11 | 5.2 | 0.0065 | 0.043 |
| 5 | BN8 | 0.052 | 0.0110 | 0.040 |
| 6 | BN9 | 0.052 | 0.0150 | 0.042 |
| 7 | BN10 | 0.052 | 0.0038 | 0.034 |
| 8 | BN11 | 0.052 | 0.0065 | 0.043 |

As mentioned before, the cooling rates were 5.2 and 0.052°C/s, respectively.

Typical BN type inclusions in directional solidification samples are shown in Fig. 9, and there are mainly single BN type inclusions and complex inclusions composited with Al₂O₃, MnS, and TiN. The morphology and the size of BN type inclusions at different cooling rates are shown in Table 6.

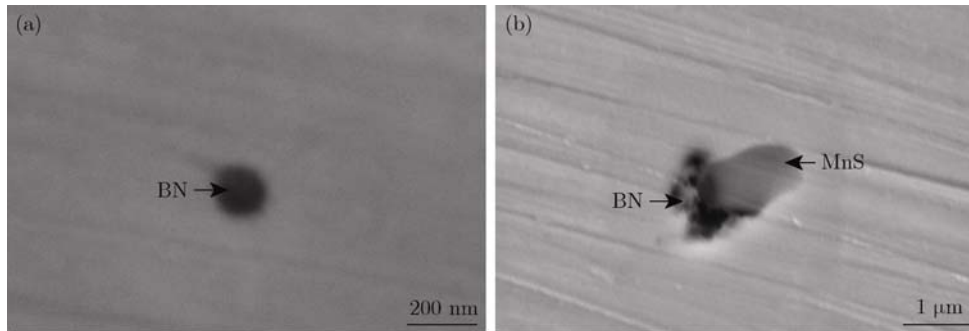


Fig. 9. Typical BN type inclusions in directional solidification samples: (a) single BN type inclusion; (b) composite BN type inclusions (with MnS).

Table 6. Morphology and size of BN type inclusions at different cooling rates

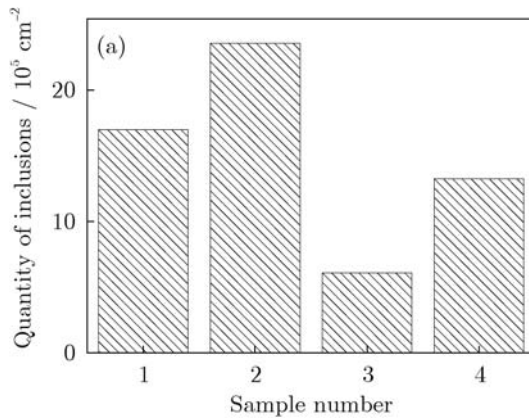
| Cooling rate / (°C·s ⁻¹) | Size / μm | | Morphology | |
|--------------------------------------|-----------|--------------|--------------------|---------------------------------------|
| | Single BN | Composite BN | Single BN | Composite BN |
| 0.052 | 1-10 | 5-20 | Spherical, cluster | Spherical, spindle, irregular polygon |
| 5.200 | <1 | None | Spherical | None |

As shown in Table 6, cooling rate has a great influence on the size of BN type inclusions. When the

cooling rate is 0.052°C/s, the morphology of BN type inclusions is multiple. When the cooling rate is 5.2

$^{\circ}\text{C}/\text{s}$, a large number of fine BN particles less than 1 μm precipitate, and the morphology is spherical. The result shows that as the cooling rate increases, the morphology of BN type inclusions becomes simpler and the size becomes smaller.

The size distribution of BN type inclusions is shown in Fig. 10 and the statistics result is shown in Fig. 11. Fig. 10 shows that when the cooling rate is $5.2^{\circ}\text{C}/\text{s}$, a large number of very fine BN inclusions precipitate in steel dispersedly because of the insufficient time of solidification. On the contrary, when the cooling rate is $0.052^{\circ}\text{C}/\text{s}$, there is enough time for BN inclusions to precipitate and grow, so BN type inclusions precipitate and grow to more than several microns. Furthermore, as the cooling rate becomes slower, groups of BN type inclusions with a larger size would be formed. The effect of B and N contents on the size of BN type inclusions is indistinctive. As shown in Fig. 11, when the



cooling rate increases, the quantity of BN type inclusions increases, and it also increases with the increase in contents of B and N in the sample.

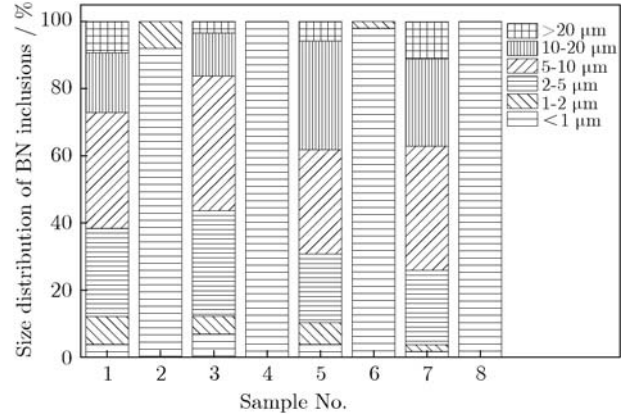


Fig. 10. Size distribution of BN type inclusions in directional solidification samples.

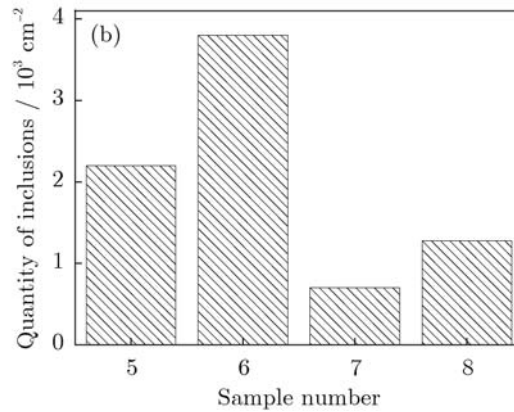


Fig. 11. Quantity of BN type inclusions in directional solidification samples at different cooling rates: (a) $5.2^{\circ}\text{C}/\text{s}$; (b) $0.052^{\circ}\text{C}/\text{s}$.

4. Conclusions

(1) In thermal equilibrium state, the maximum precipitation amount, the final precipitation amount, and the starting precipitation temperature of BN type inclusions are determined by the contents of B and N in steel. The ratio of N/B is around 1.7 when the reaction of B and N is complete in 42CrMo steel. The rapid precipitation temperature of BN type inclusions is between $1300\text{-}1400^{\circ}\text{C}$; therefore, for the precipitation of BN type inclusions, the heat treatment temperature is in this range.

(2) From the perspective of thermodynamics and kinetics, nitrides in 42CrMo steel are mainly BN and TiN, and AlN hardly generates.

(3) Cooling methods have a tremendous impact on the morphology and the size of BN type inclusions. It is presented clearly that as the cooling rate increases, the

number of large-size particles decreases and the number of small-size particles increases. The contents of B and N could hardly affect the size of BN type inclusions.

(4) As the cooling rate decreases, the quantity of BN type inclusions decreases; as the contents of B and N increase, the quantity of BN type inclusions increases.

Acknowledgements

The authors are grateful for financial supports by the National Natural Science Foundation of China (No. 51274029) and the China Postdoctoral Science Foundation (No. 2012M510319).

References

- [1] R. Tanaka, Y. Yamane, K. Sekiya, N. Narutaki, and T. Shiraga, Machinability of BN free-machining steel in turning, *Int. J. Mach. Tools Manuf.*, 47(2007), No. 12,

- p. 1971.
- [2] R. Tanaka, Y.C. Lin, A. Hosokawa, T. Ueda, and K. Yamada, Influence of additional electrical current on machinability of BN free-machining steel in turning, *J. Adv. Mech. Des. Syst. Manuf.*, 3(2009), No. 2, p. 171.
- [3] Y. Yamane, R. Tanaka, and N. Narutaki, Machinability of BN added steels, *J. Jpn. Soc. Precis. Eng.*, 64(1998), No. 9, p. 1370.
- [4] R. Tanaka, Y. Yamane, T. Ueda, A. Hosokawa, and T. Shiraga, Drilling of BN added free-machining steel, *J. Jpn. Soc. Abras. Technol.*, 52(2008), No.1, p.28.
- [5] R. Tanaka, Y. Yamane, M. Okada, A. Hosoka, and T. Ueda, End milling of free-machining steel for high speed machining, *J. Jpn. Soc. Precis. Eng.*, 73(2007), No. 7, p. 803.
- [6] C.Y. Xiang, *Alloy Structural Steels*, Metallurgical Industry Press, Beijing, 1999, p. 227.
- [7] X.F. Ding, J.P. Lin, L.Q. Zhang, Y.Q. Su, H.L. Wang, and G.L. Chen, Lamellar orientation control in a Ti-46Al-5Nb alloy by directional solidification, *Scripta Mater.*, 65(2011), No. 1, p. 61.
- [8] K. Sakuraya, H. Okada, and F. Abe, Influence of heat treatment on formation behavior of boron nitride inclusions in P122 heat resistant steel, *ISIJ Int.*, 46(2006), No. 11, p. 1712.
- [9] K. Sakuraya, H. Okada, and F. Abe, BN type inclusions formed in high Cr ferritic heat resistant steel, *Tetsu-to-Hagane*, 90(2004), No. 10, p. 819.
- [10] Q.L. Yong, *Secondary Phases in Steels*, Metallurgical Industry Press, Beijing, 2006, p. 167.
- [11] S.K. Yin, H. Komatsu, and M. Tanino, The precipitation of BN in isothermal treatment process, *Acta Metall. Sin.*, 18(1982), No. 5, p. 565.
- [12] K.C. Cho, D.J. Mun, M.H. Kang, J.S. Lee, J.K. Park, and Y.M. Koo, Effect of thermal cycle and nitrogen content on the hot ductility of boron-bearing steel, *ISIJ Int.*, 50(2010), No. 6, p. 839.
- [13] J.L. Xiao, Y.D. Guo, J.Q. Liu, S.T. Qiu, and X.Y. Li, The effect of boron on precipitation of AlN and MnS in low-carbon Al-killed steel, *J. Mater. Metall.*, 5(2006), No. 1, p. 53.
- [14] P.S. Li, L.J. Xiao, and Z. Xie, Thermodynamic analysis of AlN and BN competitive precipitation in low carbon steel, *J. Iron Steel Res.*, 21(2009), No. 5, p. 16.